Characterizing Electric Grid System Benefits of MPC-Based Residential Load Shaping

Preprint

Robert F. Cruickshank,[1] Anthony R. Florita,[2] Gregor P. Henze,[1,2] and Charles D. Corbin[3]

[1] University of Colorado
[2] National Renewable Energy Laboratory
[3] Independent consultant

Suggested Citation
Cruickshank, Robert F., Anthony R. Florita, Gregor P. Henze, and Charles D. Corbin. 2018. "Characterizing Electric Grid System Benefits of MPC-Based Residential Lad Shaping: Preprint." Golden, CO: National Renewable Energy Laboratory. NREL/CP-5D00-71539.
https://www.nrel.gov/docs/fy18osti/71539.pdf

NOTICE

CHARACTERIZING ELECTRIC GRID SYSTEM BENEFITS OF MPC-BASED RESIDENTIAL LOAD SHAPING

Robert F. Cruickshank[1], Anthony R. Florita[2], Gregor P. Henze[1,2], and Charles D. Corbin[3]

[1]University of Colorado, Department of Civil, Environmental and Architectural Engineering,
Boulder, Colorado, USA

[2]National Renewable Energy Laboratory, Power Systems Engineering Center,
Golden, Colorado, USA

[3]Consultant, Boulder, Colorado, USA

ABSTRACT

Routinely encouraging and discouraging residential electric load throughout the day will be increasingly critical in efficiently managing the smart grid to reliably deliver clean, low-cost electricity. Yet, manipulating the duty cycles of thermostatically controlled loads such as heating, air conditioning, and hot water heaters can have the effect of destabilizing or stabilizing the grid. This work explores the potential for price-responsive control of residential air conditioning to shape electric demand at the distribution feeder level to minimize electricity production costs. Physical models of the interplay between building thermal and electric loads are used to simulate time-series temperature and load behaviour. Instantaneous load-adding and load-shedding opportunities are quantified in more than 100,000 individual homes on 204 distribution feeders with results presented for 35 cities across the United States. In the context of distributed model predictive control, simulation of feeder-level response to a residential day-ahead 5-minute pricing vector to 2,146 homes highlights an aggregate impact of flexible loads.

INTRODUCTION

Considerations for the emissions and financial costs of power operations vary spatiotemporally and are driven by supply-demand interdependencies. The grid has traditionally been controlled using dispatchable generation that provides electricity to meet demand along with standby (spinning and nonspinning) reserves to meet contingencies. New controls are needed as the grid evolves and large-scale, high-inertia thermal generators are replaced by low-inertia renewable generation, particularly end-of-line and last-mile distributed generation—for example, rooftop solar photovoltaic panels.

Buildings are significant users of energy, responsible for more than 73% of the total electricity usage in the United States, with about 50% of that consumption occurring in residential buildings (EIA, 2016). As such, the ability for buildings to provide grid-controlled flexible load can be critically important as quantified by (Corbin et al. 2013, Zhao 2014, Pavlak et al. 2014).

With increasing penetrations of renewable energy sources (RES) (Henbest 2017) and waning fossil fuels in the electricity generation mix, flexible loads can help accommodate the variable and uncertain production of wind energy, solar energy, and other recent additions to the grid. Flexible loads can be used to maintain the operational balance between generation supply and user demand in transmission, distribution, and microgrids (Alstone et al. 2016, Taylor et al. 2016).

RECAP OF REDUCED-ORDER BUILDING MODEL AND MPC

To reduce electric bills, support high penetrations of RES, and achieve a host of electric grid benefits, model predictive control (MPC) has been applied in thousands of residential buildings to enable optimal supervisory control of building thermal mass through the manipulation of cooling temperature set points (Corbin 2014). Set point adjustment enables load-adding and load-shedding opportunities because additional cooling energy is stored in the thermal mass when lowered and released when raised. In the absence of grid-side control elements, such as load tap changers, distribution grid impacts were evaluated from the perspective of air-conditioning control on a single electric utility distribution feeder in three U.S. cities for the typical meteorological month of July.

The GridMPC in-home controller developed by (Corbin 2014) used a receding horizon MPC scheme to minimize an objective function of building electric energy and demand. Given that there are hundreds or thousands of buildings on a distribution feeder, the size of the decision space makes a centralized supervisory control optimization intractable. As such, a decentralized, distributed approach was adopted. Therefore, in GridMPC, a population of residential buildings was simulated as being connected to a feeder, and each performed a separate control optimization independent of the other buildings.

To improve computational efficiency and provide timely simulations, (Corbin 2014) developed a reduced-order building model (ROM), within GridMPC, suitable for determining electric load throughout the United States. The ROM combines typical meteorological year (TMY)

1

weather data, building envelope data from the Residential Energy Consumption Survey (RECS 2009), and several component models for appliances and occupancy. The RECS data were randomly sampled across several characteristics important to residential energy use, including dwelling type, floor area, envelope integrity, heating type and set point, cooling type and set point, and hot water usage. The TMY and RECS data are location specific, capturing variations from one city to another.

Using an electrical circuit analogy, all residential buildings on a representative electrical distribution feeder were expressed as a thermal network of resistive and capacitive elements. As an example, for each building the envelope model illustrated in Figure 1 consisted of six components that represented, counterclockwise from the upper left, the glazing, roof, walls, floor, internal mass, and air node.
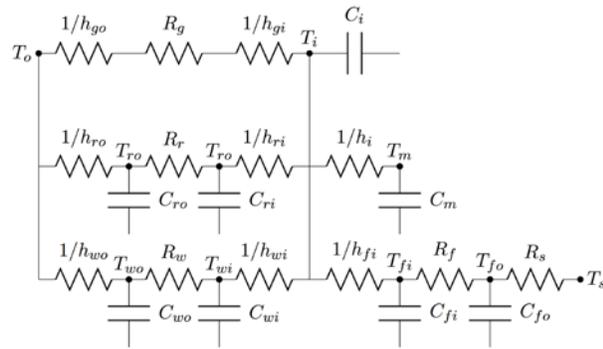

Figure 1 Building envelope model expressed as a thermal network (Corbin 2014)

For each of the solar exposed surfaces, total solar insolation was calculated from the beam, diffuse, and horizontal components. Likewise, the glazing model was a straightforward extension of the opaque surface model that included a solar heat gain coefficient. Shading by overhangs and fins was also calculated for all solar exposed surfaces. Energy balances were formulated around the individual elements shown in Figure 1 to create a system of ordinary differential equations, which were discretized in time and solved analytically. As an example, for the exterior wall node, the energy balance was expressed as:

$$\sum Q_{wo} = Q_{solwall} + h_{wo} A_w (T_o - T_{wo}) + \frac{A_w}{R_w}(T_{wi} - T_{wo}) + C_{wo}\frac{dT_{wo}}{dt}$$

where:
$\sum Q_{wo}$ is the energy balance at the outside wall node,
$Q_{solwall}$ is the energy gain caused by solar insolation,
h_{wo} is the outdoor film coefficient, and
A_w is the wall area.

A complete list of variables used in Figure 1 and Equation 1 can be found in the nomenclature section.

In addition to ordinary differential equations for the building envelope, other subsystems were modeled in (Corbin 2014). A central air-conditioning system model combined a DX air cooling coil with a constant volume fan and a dual set point thermostat that included hysteresis. Internal heat gains from equipment such as appliances and lights were modeled using a nominal energy demand, schedule, fuel type, and sensible heat fraction. The schedule value ranged from 0 to 1, representing the fraction of time that the equipment is on during a given interval. The heat gain from equipment was the energy consumed times the fraction of energy converted to heat. Heat gains from occupants were also modeled. In an annual comparison of heating and cooling loads, the ROM was found to be in agreement with EnergyPlus (BESTEST-EX), SUNREL, DOE-2.1E, and GridLAB-D (Chassin et al. 2008, Chassin et al. 2014).

In summary, the ROM of (Corbin 2014) includes an envelope model for estimating heating and cooling requirements; equipment models to calculate electric demand associated with cooling; a thermostat model to control the cooling operation; simplified end-use models (and the heat gains they produce) for appliances and electric hot water heaters. Definitions for some of these models are described in the EnergyPlus Engineering Reference (EnergyPlus 2012). Other models are largely derived from the ASHRAE HVAC 2 Toolkit (Brandemuehl 1993).

When operating as an Internet-connected smart thermostat, in the context of MPC, GridMPC adjusted set points in increments of 0.25 K, which is a typical precision of residential thermostats (Ahn and Cho 2017). GridMPC assumed each home to be unoccupied for 10 hours during the day, starting at 08:00 ±1 hour. The departure time was randomized for each home to capture occupant diversity and prevent unintended synchronization. The thermostat set point in an occupied home was altered between +0K and -2K, and in an unoccupied home between +3K and -5K. The -2K lower boundary during occupied periods recognized that larger temperature swings would likely cause occupant discomfort.

In this research, it is new and exciting that GridMPC (Corbin 2014, Corbin and Henze 2016a and 2016b) is extended by adding estimates of instantaneous electric load-adding and load-shedding opportunities at each simulation time step. This extended model allows for the creation of nationwide quantitative assessments of the impact of residential load shaping for decision and policymakers and helps quantify the electric system-wide benefits resulting from the aggregate effects of residential load shaping. Because only real power is considered

in this research, the GridLAB-D distribution simulation software used in the ROM is not used in the extended model.

SIMULATION METHODOLOGY

To simulate the impact of thermal mass-enabled residential load shaping on the distribution network in 5-minute intervals, the following steps are summarized here and further detailed next: 1) Hundreds of prototypical electric distribution feeders in cities across the United States (Schneider et al. 2008) are populated with thousands of prototypical homes (RECS 2009). 2) The ROM uses one summer's day of TMY weather data to estimate the whole-building electric demand for each residence. 3) Using the extended model, individual home's instantaneous electric load-adding/load-shedding opportunities are calculated on a 5-minute timescale based on differences between air-conditioning thermostat set points and zone temperatures. 4) Each home's electric loads and instantaneous add/shed opportunities are aggregated to the feeder level. 5) Feeder loads and instantaneous add/shed opportunities are aggregated to the city level. 6) As a separate activity, GridMPC uses 5-minute day-ahead forecast pricing to control air-conditioning load, in the context of distributed MPC, to simulate a single feeder-level response to residential load shaping.

Step 1) Using data from the (RECS 2009), the MATLAB feeder generation scripts provided by the GridLAB-D development team are used to automatically generate a population of residential buildings based on feeder nominal load characteristics and climate region.

Step 2) For each house, a base case load simulation involves the following: A) A fixed cooling temperature set point is selected from a distribution. B) Using TMY and RECS data, the zone free-float temperature for the current time period is found by simulating without operating air conditioning equipment. C) If the zone temperature exceeds the cooling set point, the energy required to bring the zone back to the temperature is calculated; if not, new mass and zone temperatures are calculated. D) Energy consumption by the air-conditioning equipment is calculated given the delivered cooling energy from each time step. The ROM is used for the calculations in steps (B) through (D). The base case load includes air-conditioning, miscellaneous electric loads, appliances, and electric hot water heaters. Alternatively, other than base case simulation, Step 2 can be modified to simulate a load-shaping ancillary service that is provided by Grid-MPC set point adjustment in response to forecast pricing.

Step 3) For each house, using the extended model, the calculation of the zone temperature in each time step enables a logic-based assessment of whether the conditioned space is at the upper or lower temperature limits of comfort. Subject to minimum run-time constraints, if the air conditioner is *off* and the zone temperature is between comfort limits, then load can be added. Similarly, if the air conditioner is *on* and the zone temperature is between comfort limits, then load can be shed. However, if the zone temperature is at the upper comfort limit, then no load can be shed because the air conditioner must run; likewise, if the zone temperature is at the lower comfort limit, then no load can be added without overcooling the zone. This *on/off* logic governs the calculation of instantaneous load-adding/load-shedding opportunities within temperature set points.

Step 4) Residential loads and instantaneous add/shed opportunities are aggregated at the feeder level using the R statistical programming environment (R 2018). Instantaneous add/shed opportunities in *MW* are then divided by feeder demand in *MW* and expressed as a percentage of feeder load.

Step 5) The percentage load add/shed results are transformed into a weighted average (on a per city basis) by multiplying the output of Step 4 by the percentage of each type of feeder per city. To create a nationwide perspective of instantaneous load-adding/load-shedding opportunities, multiple representative feeders are simulated in nearly equally spaced cities across the climate regions defined in the distribution taxonomy in (Schneider et al. 2008). For reference, a map of distribution taxonomy climate regions is shown in Figure 2, and a list of feeder weighting and characteristics are shown in Table 1.

It is critically important to note that following a load-adding/load-shedding event, the future operation of air conditioning cannot be controlled continuously. The resulting load-adding and load-shedding opportunities after participating in load increase and decrease events is discussed in Step 6.

Step 6) Last, GridMPC evaluates the time-varying load-shaping capabilities of homes reacting to a day-ahead 5-minute electricity pricing forecast. A perfect forecast is assumed that is based on recent residential market-cleared prices from, for example, the ComEd Internet API (Commonwealth 2018). The ComEd Chicago market prices used in this simulation are illustrative only and are not representative of the rest of the United States. That said, just as per-city TMY data are available today, in the future it is expected that location-based forecast marginal pricing will also be available—and will be a critical spatiotemporal input that is used to automatically shape residential load to provide ancillary services throughout the distribution and transmission grid.
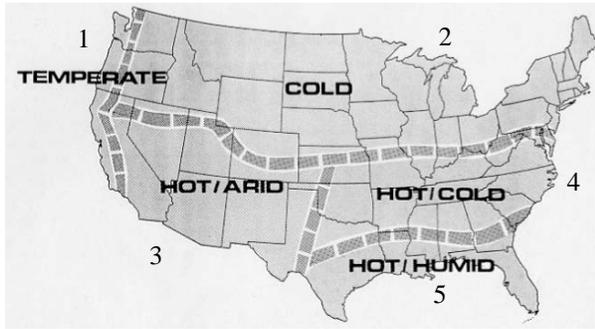
3

Figure 2. Regional climate characteristics (adapted from Schneider et al. 2008).

Table 1 Prototypical feeder weighting by region

Region	Feeder	kV	# of Feeders	% within a Region	Description
Region 1	R1-12.47-1	12.5	2,200	21%	Moderate suburban and rural
	R1-12.47-2	12.47	2,500	23%	Moderate suburban and light rural
	R1-12.47-3	12.47	2,000	19%	Small urban center
	R1-12.47-4	12.47	1,800	17%	Heavy suburban
	R1-25.00-1	24.9	1,200	11%	Light rural
	GC-12.47-1	12.47	1,000	9%	Single large commercial or industrial
	Total		10,700		
Region 2	R2-12.47-1	12.5	3,500	19%	Light urban
	R2-12.47-2	12.47	3,200	17%	Moderate suburban
	R2-12.47-3	12.47	3,000	16%	Light suburban
	R2-25.00-1	24.9	3,500	19%	Moderate urban
	R2-35.00-1	34.5	4,000	21%	Light rural
	GC-12.47-1	12.47	1,500	8%	Single large commercial or industrial
	Total		18,700		
Region 3	R3-12.47-1	12.47	1,500	30%	Heavy urban
	R3-12.47-2	12.47	1,500	30%	Moderate urban
	R3-12.47-3	12.47	1,000	20%	Heavy suburban
	GC-12.47-1	12.47	1,000	20%	Single large commercial or industrial
	Total		5,000		
Region 4	R4-12.47-1	13.8	1,400	33%	Heavy urban with rural spur
	R4-12.47-2	12.5	1,500	36%	Light suburban and moderate urban
	R4-25.00-1	24.9	1,250	30%	Light rural
	GC-12.47-1	12.47	750	2%	Single large commercial or industrial
	Total		4,900		
Region 5	R5-12.47-1	13.8	400	9%	Heavy suburban and moderate urban
	R5-12.47-2	12.47	600	13%	Moderate suburban and heavy urban
	R5-12.47-3	13.8	650	14%	Moderate rural
	R5-12.47-4	12.47	500	11%	Moderate suburban and urban
	R5-12.47-5	12.47	450	10%	Moderate suburban and light urban
	R5-25.00-1	22.9	450	10%	Heavy suburban and moderate urban
	R5-35.00-1	34.5	500	11%	Moderate suburban and light urban
	GC-12.47-1	12.47	1,000	22%	Single large commercial or industrial
	Total		4,550		

DISCUSSION AND RESULT ANALYSIS

A. Single Residence Load Shaping Opportunities

An example of GridMPC load management optimization of residential central air-conditioning reveals adjustments to the cooling set point throughout July 20, as shown in Figure 3. Note the smaller changes in set point when the home is occupied and the larger changes in set point during the middle of the day when the home is expected to be unoccupied.
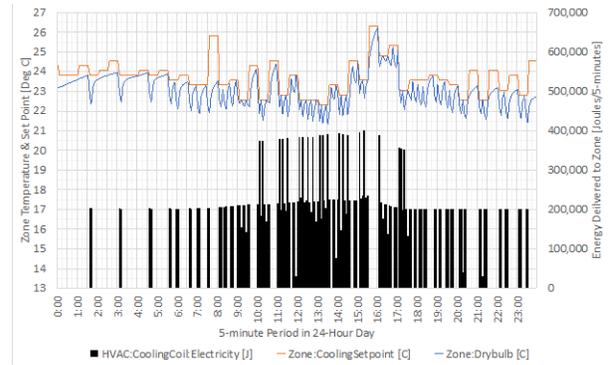
Figure 3 GridMPC air-conditioning set point in gold, zone temperature in blue, and energy delivered in black every 5 minutes, assuming a two-stage central air-conditioning system with a 10-minute minimum run time

Applying the temperature comfort constraint logic, Figure 4 shows the instantaneous load adding/load-shedding opportunities for the house every 5 minutes on July 20.
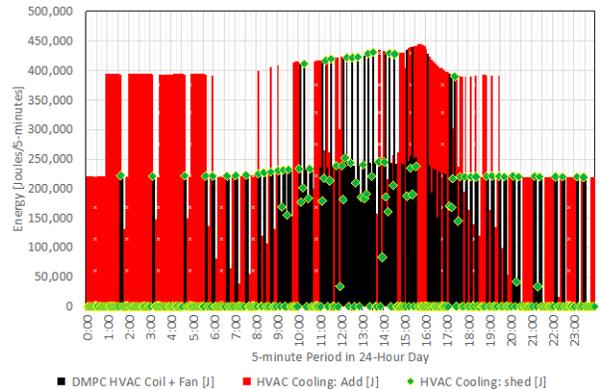
Figure 4 Thermal mass-enabled instantaneous load-adding/load-shedding opportunities for a single-family house every 5-minutes. As in Figure 3, black denotes air-conditioning load. Red denotes load-adding opportunities, and green diamonds denote load-shedding opportunities. Note that because of comfort constraints, there are a few intervals when load cannot be added and many intervals when load cannot be shed.

B. Feeder-Level Load Shaping Opportunities

To calculate base case feeder-level instantaneous load opportunities, fixed set points are constant in time, and add/shed results are aggregated every 5 minutes across 2,146 homes on the Houston prototypical Feeder 22, as shown in Figure 5. The red area depicts load-adding opportunities, with the top being the maximum possible instantaneous load. The top of the black area is the base case whole-building load. The black region depicts load-shedding opportunities, with the minimum possible instantaneous load depicted by the top of the green area.

4

Figure 5 Thermal mass-enabled instantaneous feeder load adding/shedding based on aggregated whole-building electric use

Figure 6 Thermal mass-enabled instantaneous feeder load adding/shedding, expressed as percentage, based on aggregated whole-building electric use

After normalizing feeder-level results, Figure 6 shows the average percentage instantaneous load adding/load-shedding opportunities as a function of whole-building electric load every 5-minutes on July 20 based on the same 2,146 homes on Houston Feeder 22.

The results of combining feeder-level instantaneous load-adding/load-shedding opportunities on per city basis across the United States on July 20 are shown in Figure 7. Distributional statistics of the colours at left are depicted in the table values at right. Nationwide summary statistics appear at lower right.
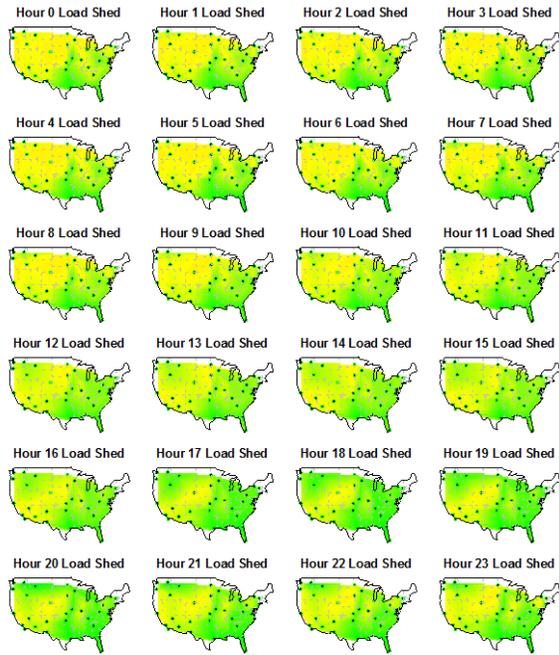

City	State	Min	Max	Avg	Min	Max	Avg
ALBANY	NY	-18	0	-7	23	68	40
ALBUQUERQUE	NM	-16	0	-7	2	34	18
ATLANTA	GA	-31	0	-17	13	123	49
BALTIMORE	MD	-30	-1	-13	17	95	41
BOISE	ID	-34	0	-12	15	111	36
CHARLESTON	WV	-30	-4	-23	8	101	45
CHEYENNE	WY	-18	0	-4	0	36	13
CHICAGO	IL	-32	-1	-14	22	84	46
DETROIT	MI	-31	-1	-15	19	124	45
EL_PASO	TX	-12	-1	-8	3	35	17
FARGO	ND	-24	0	-6	2	81	25
HELENA	MT	-32	0	-13	5	123	30
HOUSTON	TX	-53	-6	-36	23	189	88
JACKSONVILLE	FL	-43	-4	-32	12	166	73
KANSAS_CITY	MO	-32	-5	-26	15	121	49
LAS_VEGAS	NV	-8	-1	-6	2	22	10
LOS_ANGELES	CA	-6	0	-3	2	20	7
MIAMI	FL	-31	-4	-26	14	109	50
MINNEAPOLIS	MN	-29	0	-13	12	121	34
MOBILE	AL	-36	-3	-27	11	131	58
NASHVILLE	TN	-35	-1	-17	15	149	48
NEW_YORK_CITY	NY	-32	-2	-19	14	131	50
OKLAHOMA_CITY	OK	-32	-3	-24	12	115	51
PHOENIX	AZ	-13	-1	-10	4	34	17
PITTSBURGH	PA	-34	-1	-15	19	89	54
PORTLAND	ME	-18	0	-5	1	40	14
RICHMOND	VA	-30	-2	-19	13	108	44
SAN_DIEGO	CA	-12	-1	-7	4	33	14
SAN_FRANCISCO	CA	-11	0	-3	0	38	13
SEATTLE	WA	-21	0	-7	1	46	15
SIOUX_FALLS	SD	-8	0	-3	0	23	7
SPOKANE	WA	-33	-1	-19	4	120	40
ST_LOUIS	MO	-13	0	-5	14	44	23
SYRACUSE	NY	-30	0	-12	14	74	32
WICHITA	KS	-14	0	-8	10	55	23
		Min	Max	Avg	Min	Max	Avg
←— Load Shed —→	←— Load Add —→	-53	0	-14	0	189	35

Figure 7 Heat map of thermal mass-enabled U.S. residential air-conditioning instantaneous percentage electric load-adding/load-shedding opportunities every 5 minutes. Note the increased add/shed opportunities because of increased air-conditioning loads in hot and humid southern climates, e.g., Houston, Texas, and Jacksonville, Florida

Figure 8 represents the corresponding instantaneous load-shedding opportunities during the 5-minute interval at the top of each hour for all 24 hours of July 20. The colours in Figure 8 reference the minimum and maximum scale of -53% to 0% load shed depicted in the lower right of Figure 7.

5

Figure 8 U.S. load <u>shed</u> contour map for all hours of a summer day. Green indicates increased ability to shed

Figure 9 represents the corresponding load-<u>adding</u> opportunities during the 5-minute interval at the top of each hour for all 24 hours of July 20. The colours in Figure 9 reference the minimum and maximum scale of 0% to 189% load add depicted in the lower right of Figure 7.
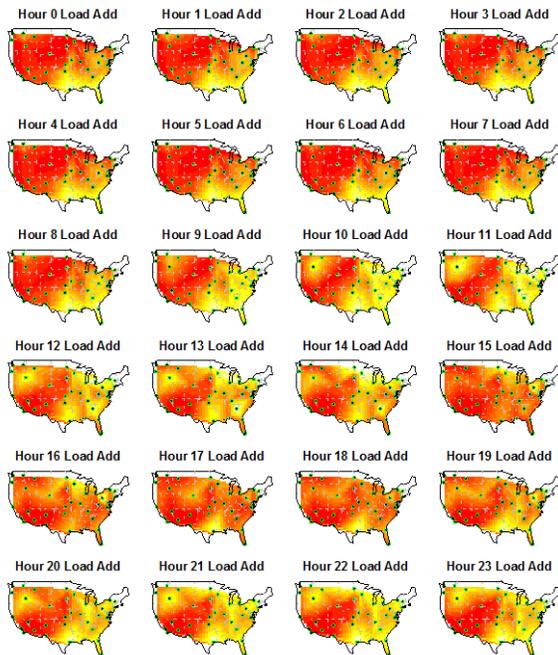

Figure 9 U.S. load <u>add</u> contour map for all hours of a summer day. Red indicates increased ability to add

The amount of add/shed opportunities over time is proportional to the duty cycle of air-conditioning systems. An air conditioner with a low duty cycle (in cooler hours) has a low opportunity to shed load and high opportunity to add load. Conversely, an air conditioner with a high duty cycle (in warmer hours) has a high opportunity to shed load and a low opportunity to add load.

The magnitude of add/shed opportunities is proportional to the size of air conditioners. The larger air conditioners required in hot climates have larger compressors and circulation motors and hence provide increased add/shed magnitudes.

C. Feeder-Level MPC Control Response

The final step was evaluating the MPC load-shaping capabilities of 100% participating homes based on an assumed perfect forecast of day-ahead residential 5-minute pricing starting at midnight. Simulation results of deviations are shown in Figure 10, depicting base case and optimized loads every 5 minutes on July 20 based on the same 2,146 homes on Houston Feeder 22. Note that, in practice, price fluctuations and building responses would be based on the balance of system needs, not on Chicago market pricing. Also note that any air-conditioning set point adjustment has time-lagged effects because the aggregate building responses are slower than the 5-minute price changes.
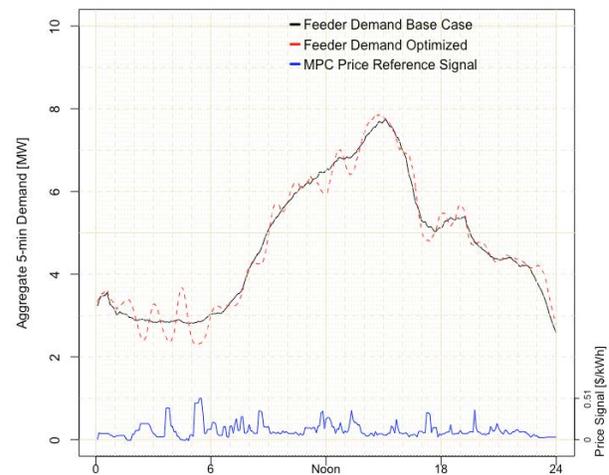

Figure 10 Single-day feeder-level response. Base case demand is shown in black. The MPC-based response to forecast price signal is shown in red. Midnight-to-midnight 5-minute forecast price signal is shown in blue. Note the reductions in demand during high price periods. Depending on the needs of the grid, the oscillatory nature can be good for providing grid ancillary services, but it might be bad for air conditioners that are cycled on and off too frequently

6

As shown in Figure 11, residential electric rates vary by a multiple of 3 or more across the United States, highlighting the spatiotemporal nature and potential value of flexible residential building loads (Open EI 2018).
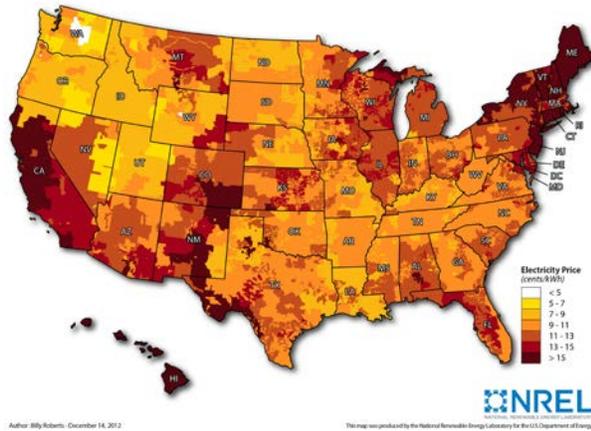

Figure 11 U.S. residential electric rates in 2012

CONCLUSION

This study contributes to characterizing electric grid system benefits of MPC-based residential load shaping. The spatiotemporal potential is explored across the United States for residential buildings to shape electric demand at the distribution feeder level by adding or shedding load to minimize electricity production costs. Air-conditioning and appliance loads in more than 100,000 homes on 204 distribution feeders are calculated based on TMY weather data and a thermal house model that reflects geographic diversity in the building stock. A weighted average of feeders is used to express results for 35 cities. Depending on the city and 5-minute interval, thermal mass-enabled load-shedding opportunities up to 53% of load are possible, and load-adding opportunities up to 189% of load are possible. Instantaneous load-adding/load-shedding opportunities caused by air-conditioning are depicted as a function of geographical location and time of day. Also included is a 24-hour simulation of feeder response to a residential day-ahead perfect forecast 5-minute pricing signal in the context of distributed MPC of air-conditioning load.

Future research will investigate the impact of including additional degrees of freedom in residential load control, including electric hot water heating and battery storage, along with estimates of reductions in production costs, wholesale prices, and emissions. Scenarios will include the presence of forecast pricing and time-of-use price tariffs for different U.S. regions.

NOMENCLATURE

In the building envelope expressed as a thermal model, for the glazing:

T_i is the zone dry-bulb temperature,
h_{gi} is the interior film coefficient,
R_g is the glass thermal resistance,
h_{go} is the outdoor film coefficient, and
T_o is the outdoor dry-bulb temperature.

For the roof:
h_{ri} is the interior film coefficient,
T_{ri} is the interior roof dry-bulb temperature,
C_{ri} is the interior roof thermal capacitance,
R_r is the roof thermal resistance,
T_{ro} is the outdoor roof dry-bulb temperature,
C_{ro} is the outdoor roof thermal capacitance, and
h_{ro} is the outdoor film coefficient.

For the walls:
h_{wi} is the interior film coefficient,
T_{wi} is the interior wall dry-bulb temperature,
C_{wi} is the interior wall thermal capacitance,
R_w is the wall thermal resistance,
T_{wo} is the outdoor wall dry-bulb temperature,
C_{wo} is the outdoor wall thermal capacitance, and
h_{wo} is the outdoor film coefficient.

For the floor:
h_{fi} is the interior film coefficient,
T_{fi} is the interior floor dry-bulb temperature,
C_{fi} is the interior floor thermal capacitance,
R_f is the floor thermal resistance,
T_{fo} is the outdoor floor dry-bulb temperature,
C_{fo} is the outdoor floor thermal capacitance,
R_s is the soil thermal resistance, and
T_s is the deep soil temperature.

For the internal mass in the zone:
h_i is the interior film coefficient,
T_m is the mass dry-bulb temperature, and
C_m is the mass thermal capacitance.

For the zone, C_i is the thermal capacitance.

REFERENCES

Ahn, J. and Cho, S. 2017. "Dead-band vs. machine-learning control systems: Analysis of control benefits and energy efficiency," J Build Eng, vol. 12, pp. 17–25.

Alstone, P. et al. 2016. 2025 California Demand Response Potential Study. Lawrence Berkeley National Laboratory

Brandemuehl, Michael J. 1993. HVAC 2 Toolkit: A Toolkit for Secondary HVAC System Energy Calculations. American Society of Heating, Refrigerating and Air-Conditioning Engineers, Atlanta, Georgia.

Chassin, D.P., Schneider, K., Gerkensmeyer, C. 2008. GridLAB-D: An Open-Source Power Systems Modelling and Simulation Environment, IEEE 2008 PES Transmission and Distribution Conference and Exposition, 21-24 April 2008. http://dx.doi.org/10.1109/TDC.2008.4517260

Chassin, D. P., Fuller, J., C., Djilali, N. 2014. GridLAB-D: An Agent-Based Simulation Framework for Smart Grids, Journal of Applied Mathematics, vol. 2014, Article ID 492320, 12 pages, http://dx.doi.org/10.1155/2014/492320

Commonwealth Edison. 2018, 5-minute price data API, https://hourlypricing.comed.com/hp-api/

Corbin, C. D. 2014. Assessing Impact of Large Scale Distributed Residential HVAC Control Optimization and Electricity Grid Operation and Renewable Energy Integration, University of Colorado, Boulder, CO.

Corbin, C. D. Henze, G. P. 2016. Predictive Control of Residential HVAC and its Impact on the Grid. Part I: Simulation Framework and Models. Journal of Building Performance Simulation, DOI: 10.1080/19401493.2016.1231220

Corbin, C. D. Henze, G. P. 2016. Predictive Control of Residential HVAC and its Impact on the Grid. Part II: Simulation Studies of Residential HVAC as a Supply Following Resource. Journal of Building Performance Simulation, DOI: 10.1080/19401493.2016.1231221

Corbin, C.D., Henze, G. P., May-Ostendorp, P. A. 2013. A Model Predictive Control Optimization Environment for Real-Time Commercial Building Application. Journal of Building Performance Simulation, 6:3, 159-174, DOI: 10.1080/19401493.2011.648343

EIA 2016. Electric Power Annual 2015, Energy Information Administration, https://www.eia.gov/electricity/annual/pdf/epa.pdf

EnergyPlus Engineering Reference: The Reference to EnergyPlus Calculations. 2012. United States Department of Energy.

Henbest, S. 2017. New Energy Outlook, Bloomberg New Energy Finance, https://about.bnef.com/new-energy-outlook

Pavlak, G.S. Henze, G. P., Cushing, V. J. 2014. Optimizing Commercial Building Participation in Energy and Ancillary Service Markets. Energ Buildings, 81:115–126.

OpenEI 2018. Residential Electric Rates, https://openei.org/w/images/6/60/2012_12_14_Electricity_Price-01.jpg

U.S. Energy Information Administration. 2009. Residential Energy Consumption Survey (RECS). http://www.eia.gov/consumption/residential/

Ron Judko, Ben Polly, Marcus Bianchi, and Joel Neymark. Building Energy Simulation Test for Existing Homes (BESTEST-EX) Phase 1 Test Procedure: Building Thermal Fabric Cases. Technical report, National Renewable Energy Laboratory, Golden, Colorado, 2010.

Schneider, K. P., Chen, Y, Chassin, D. P., Pratt, R., Engel, D. W., Thompson, S. 2008. Modern Grid Initiative Distribution Taxonomy Final Report, Pacific Northwest National Laboratory, PNNL-18035

Taylor, JA, Dhople, SV and Callaway, DS 2016. Power systems without fuel. Renewable and Sustainable Energy.

The R Project for Statistical Computing. 2018. https://www.r-project.org

Zhao, P. 2014. Dynamic Building-to-Grid integration through combined building system resources for frequency regulation service, University of Colorado, Boulder, CO.